Cross section and asymmetry parameter calculations for the C 1*s* photoionization of CH_4, CF_4, and CCl_4

Alexandra P. P. Natalense and Luiz M. Brescansin
Instituto de Física Gleb Wataghin, Universidade Estadual de Campinas, Unicamp, 13083-970 Campinas, São Paulo, Brazil

Robert R. Lucchese
Department of Chemistry, Texas A&M University, College Station, Texas 77843-3255, USA

(Received 5 May 2003; published 4 September 2003)

We have computed cross sections and asymmetry parameters for the C 1*s* photoionization of CX_4 (X = H, F, Cl) using the Schwinger variational method with Padé corrections. We present a comparative study that shows the influence of the identity of the X atom on the computed cross sections. Predicted cross sections are in good agreement with available photoionization and photoabsorption experimental data. We conclude that the presence of heavy outer atoms produces resonance structures in the photoionization cross sections and in the asymmetry parameters. We find a single nonvalence resonant state in the photoionization of CF_4 and multiple resonances in CCl_4 that have significant *d*-orbital character in the vicinity of the Cl atoms.

DOI: 10.1103/PhysRevA.68.032701 PACS number(s): 33.80.Eh

I. INTRODUCTION

Quantitative information on the interaction of photons with molecules such as CH_4, CF_4, and CCl_4 are of fundamental and practical interest. The two halogenated methane compounds cited above, among others, play an important role in the depletion of Earth's ozone layer [1]. Methane itself is an important planetary atmosphere constituent of outer planets such as Uranus and Neptune [2] and is one of the many gases that contribute to the development of the greenhouse effect [3]. It has also become a useful and interesting test system for theoreticians since it is one of the simplest polyatomic molecules.

The Schwinger variational method (SVM) has been applied successfully to the study of the photoionization of several molecules, within many different levels of approximation. Some of the most recent applications for linear molecules include the frozen-core Hartree-Fock result for N_2 [4], the relaxed-core Hartree-Fock calculation for CO [5], the multichannel configuration-interaction approximation for CO [6], C_2H_2 [7,8], and for N_2 [9], which also include a complete active space configuration-interaction approximation. Years ago, the SVM was implemented for C_{2v} molecules (H_2O [10]) and for molecules that have a point group which has C_{2v} as a subgroup (SiH_4 [11] and C_2H_4 [12]). Recently the SVM was generalized for polyatomic molecules of arbitrary symmetry, producing very good results for the S 1*s* photoionization of SF_6 [13], and the valence photoionization of C_{60} [14].

In this paper we present C 1*s* cross sections and asymmetry parameters for the photoionization of the systems CH_4, CF_4, and CCl_4 using the polyatomic Schwinger variational method with Padé corrections. There have been several studies on the photoabsorption of CH_4 [15–17], CF_4 [15,17–20], and CCl_4 [19,21]. There is also an extensive bibliography and database available for inner-shell processes including those considered here [22]. However, to our knowledge, only for CF_4 have theoretical [23] and experimental [24] results on the photoionization of the C 1*s* level been reported.

The version of the SVM that we use here is essential a one-electron method. Thus in the computed cross sections we will only see effects due to one-electron processes. Thus in the study of core photoionization, we will not find any autoionization resonance structures or effects due to interchannel coupling to shake-up channels [25]. The resonance processes we will find are shape resonances. In molecular photoionization, shape resonances are primarily due to dynamical angular-momentum barriers [26]. Thus resonance wave functions are usually characterized by high angular-momentum states as seen through the structure of their nodal surfaces. A high angular-momentum barrier leads to high resonance energies and/or narrow resonances. Thus in the photoionization of SF_6, a resonant state that asymptotically corresponds to $l=9$ angular momentum is found to have photoelectron kinetic energy of 57 eV [13], whereas a resonant state in the photoionization of N_2 with asymptotic angular momentum of $l=3$ has a photoelectron kinetic energy of 15 eV [26,27]. In molecular systems, the resonant states can also be characterized by the degree to which the wave function can be constructed by atomic centered valence orbitals. In general, some of the resonant states appear to be similar to the unoccupied states in a simple valence molecular-orbital picture of the electronic structure of the molecule, while others have a nonvalence character. Thus in the C 1*s* ionization of the three tetrahedral molecule considered here, one must consider the unoccupied valence states of t_2 symmetry. In CH_4 and CF_4 there is one unoccupied σ^*(C-X) orbital of t_2 symmetry. In CH_4, the H nuclei do not have an attractive enough interaction with the photoelectron to support a shape resonance. In CF_4, the C $1s \rightarrow \sigma^*$(C-X) states are believed to occur below the C 1*s* ionization threshold [19,23] and thus would not appear in the ionization continuum. Thus any shape resonance in the C 1*s* ionization of CF_4 would be due to a nonvalence state. In CCl_4 there would

be both σ^*(C-X) orbitals of t_2 symmetry as well as states that can be formed from the valence $3d$ atomic orbitals on the Cl atoms. In the case of CCl_4 the C1$s \rightarrow \sigma^*$(C-X) states are again expected to occur below the C $1s$ ionization threshold [19]. However, we still might expect to see shape resonances that have wave functions which have a d-orbital character around the Cl atoms.

The organization of this paper is as follows: In Sec. II we describe the main features of the theoretical method. Section III presents the computational details of our calculations. Our results are shown in Sec. IV and our conclusions are summarized in Sec. V.

II. METHOD

The details of our method were described elsewhere [13,28,29], so only some of its main features will be reviewed here. The differential cross section, averaged over the molecular orientations, is given by

$$\frac{d\sigma^{(L,V)}}{d\Omega_k} = \frac{\sigma^{(L,V)}}{4\pi}[1+\beta_k^{(L,V)}P_2(\cos\theta)], \tag{1}$$

where the total cross section $\sigma^{(L,V)}$ is

$$\sigma^{(L,V)} = \frac{4\pi^2}{3c}E\sum_{p\mu lh v}|I^{(L,V)}_{klhv,p\mu}|^2 \tag{2}$$

and where (L,V) stands for either the length (L) or velocity (V) form of the cross section. In Eq. (2), p is one of the irreducible representations of the molecular point group, μ is a component of the representation p, h indexes the different functions belonging to the same irreducible representation $(p\mu)$ with the same value of l, v designates components of the dipole moment operator, E is the photon energy, k is the magnitude of the momentum of the photoelectron, and c is the speed of light.

In Eq. (1), the asymmetry parameter β can be written as [10]

$$\begin{aligned}\beta_k^{(L,V)} = \frac{3}{5}&\frac{1}{\sum_{p\mu lhv}|I^{(L,V)}_{klhv,p\mu}|^2}\\ &\times\sum_{\substack{p\mu lhvmm_v\\ p'\mu' l'h'v'm'm'_v}}(-1)^{m'-m_v}I^{(L,V)}_{klhv,p\mu}(I^{(L,V)}_{kl'h'v',p'\mu'})^*\\ &\times b^{p\mu}_{lhm}b^{p'\mu'*}_{l'h'm'}b^{p_v\mu_v}_{1vm_v}b^{p'_v\mu'_v*}_{1v'm'_v}[(2l+1)(2l'+1)]^{1/2}\\ &\times\langle 1100|20\rangle\langle l'l00|20\rangle\langle 1,1,-m'_v,m_v|2,M'\rangle\\ &\times\langle l',l,-m',m|2,-M'\rangle,\end{aligned} \tag{3}$$

where the $\langle l'lm'm|L'M'\rangle$ are the usual Clebsch-Gordan coefficients and the $b^{p\mu}_{lhm}$ are expansion coefficients that define the functions $\chi^{p\mu}_{lh}$, which are the symmetry-adapted angular expansion functions [30] that are related to the usual spherical harmonics by

$$\chi^{p\mu}_{lh}(\theta,\phi) = \sum_m b^{p\mu}_{lhm}Y_{lm}(\theta,\phi). \tag{4}$$

The quantities $I^{(L,V)}_{klhv,p\mu}$ appearing in Eqs. (2) and (3) are the partial-wave components of the dynamical coefficients $I^{(L,V)}_{\mathbf{k},\hat{\boldsymbol{n}}}$ [10],

$$I^{(L,V)}_{\mathbf{k},\hat{\boldsymbol{n}}} = \left(\frac{4\pi}{3}\right)^{1/2}\sum_{p\mu lhv}I^{(L,V)}_{klhv,p\mu}\chi^{p\mu}_{lh}(\hat{\boldsymbol{k}})\chi^{p_v\mu_v}_{1v}(\hat{\boldsymbol{n}}), \tag{5}$$

where

$$I^{L}_{\mathbf{k},\hat{\boldsymbol{n}}} = (k)^{1/2}\langle\Psi_i|\mathbf{r}\cdot\hat{\boldsymbol{n}}|\Psi^{(-)}_{f,\mathbf{k}}\rangle \tag{6}$$

for the dipole length form and

$$I^{V}_{\mathbf{k},\hat{\boldsymbol{n}}} = \frac{(k)^{1/2}}{E}\langle\Psi_i|\boldsymbol{\nabla}\cdot\hat{\boldsymbol{n}}|\Psi^{(-)}_{f,\mathbf{k}}\rangle \tag{7}$$

for the dipole velocity form. In the above equations, Ψ_i is the target ground-state wave function, $\Psi^{(-)}_{f,\mathbf{k}}$ is the final continuum state wave function (with incoming-wave boundary condition) of the system (ion plus photoelectron), $\mathbf{k}$ is the photoelectron momentum, and $\hat{\boldsymbol{n}}$ represents the unit vector in the direction of polarization of the radiation, which is assumed to be linearly polarized.

Calculations using the dipole length and velocity forms of the dynamical coefficient would produce the same results if the exact wave functions were used. Since the wave-function calculation involves the use of approximations, the differences between the results of Eqs. (6) and (7) can be used as a test of the quality of our wave function. In the calculations reported here, we use the mixed form, so that the differential cross section is given by [31]

$$\frac{d^2\sigma^M}{d\Omega_{\hat{\mathbf{k}}}d\Omega_{\hat{\boldsymbol{n}}}} = \frac{4\pi^2E}{c}\mathrm{Re}\{[I^{\mathrm{L}}_{\mathbf{k},\hat{\boldsymbol{n}}}]^*I^{\mathrm{V}}_{\mathbf{k},\hat{\boldsymbol{n}}}\}. \tag{8}$$

The cross sections obtained in the mixed form usually lie between the ones produced by the length and velocity forms [32].

We use the single-center expansion method [28] in the solution of the scattering problem. In this method, all three-dimensional functions are expanded in the set of angular symmetry-adapted functions $\chi^{p\mu}_{lh}(\theta,\phi)$, defined in Eq. (4), according to the irreducible representations of the molecular point group (T_d for the three molecules studied here). An arbitrary three-dimensional function $F^{p\mu}(r,\theta,\phi)$ is then expanded as

$$F^{p\mu}(r,\theta,\phi) = \sum_{lh} r^{-1}f^{p\mu}_{lh}(r)\chi^{p\mu}_{lh}(\theta,\phi), \tag{9}$$

where the radial functions $f_{lh}^{p\mu}(r)$ are represented on a numerical grid. When solving the scattering equations we enforce orthogonality between the continuum solutions and the occupied orbitals [33].

In the present study, the initial neutral molecule electronic wave function Ψ_i and the final ionized molecule electronic wave function are described by single Slater determinants constructed using the Hartree-Fock orbitals of the initial neutral state. The ionic orbitals are then constrained to be identical to those of the initial ground state. Our approximation does not include the effect of relaxation of the ion due to the localized nature of the core hole, which is known to affect the position, width, and magnitude of resonances [34]. With this approximation we reduce the computation of the final photoionization problem to solving the problem of an electron under the action of the potential of the molecular ion. We then do not consider many-electron correlation effects, although we do include the nonlocal exchange interaction which is a consequence of the many-electron nature of the states involved. The photoelectron orbital is a solution of the one-electron Schrödinger equation [33] (in atomic units):

$$\left[-\frac{1}{2}\nabla^2+V(\mathbf{r})-\frac{k^2}{2}\right]\psi_{\mathbf{k}}^{(\pm)}(\mathbf{r})=0, \tag{10}$$

where $V(\mathbf{r})$ is the static-exchange potential [13], and $\psi_{\mathbf{k}}^{(\pm)}(\mathbf{r})$ satisfies appropriate boundary conditions. We could include correlation and polarization effects in our calculations through the addition of a local, energy-independent, model correlation polarization potential (as described in Ref. [29]), but as in the case of the S 1*s* photoionization of SF_6 [13], we found that such a polarization potential does not significantly affect our final results for the C 1*s* photoionization of CH_4, CF_4, and CCl_4.

To proceed, Eq. (10) is rewritten in an integral form, the Lippmann-Schwinger equation, and is solved using an iterative procedure based on the Schwinger variational principle and Padé approximants. This method provides photoionization matrix elements that have been found to converge to the exact values for a given projectile-target interaction potential [13,29].

We have studied some of the resonance structures found in our calculated cross sections using the local adiabatic static model exchange method (ASME) [26]. In this method we use a simplified model potential and we do not include orthogonality constraints. The resonant energies are then determined by locating the poles of the scattering matrix that has been analytically continued to complex energies. Once the resonance energy is found the corresponding resonance wave function can be computed and analyzed. The ASME calculations allow for a qualitative understanding of the main features of the resonant process by including sufficient details of the full scattering problem, but using a potential form that makes the analytic continuation feasible. The ASME method has been successfully applied to photoionization [13] and electron-scattering [26] studies.

TABLE I. Interatomic distances (Å) and self-consistent field (SCF) energies (hartrees).

Molecule	Distance	SCF energy (this work)	SCF energy (from the literature)
CH_4	1.091 [44]	−40.21027	−40.1987 [45,46]
CF_4	1.323 [47]	−435.78392	−435.76699 [29]
CCl_4	1.767 [47]	−1875.87501	

III. COMPUTATIONAL DETAILS

Our molecular targets were represented within the Hartree-Fock approximation using the 6-311G basis set from the GAUSSIAN98 code [35], augmented with two sets of *d* polarization functions on the heavy atoms for all three molecules. At the experimental equilibrium ground-state distances of CH_4, CF_4, and CCl_4 this basis set produces the self-consistent field energies shown in Table I, where we also compare them to other values available in the literature. All calculations were carried out in the fixed-nuclei approximation. To calculate the matrix elements of Eqs. (6) and (7) we only need to compute the final continuum states $|\Psi_{f,\mathbf{k}}^{(-)}\rangle$ belonging to the T_2 symmetry, since the three components of the dipole operator transform as the T_2 irreducible representation of the T_d point group. Since the C 1*s* hole states have A_1 symmetry in all of these molecules, the continuum orbitals will also have t_2 symmetry. The photon energies in the calculations were obtained using the experimental ionization potentials for the C 1*s* ionization which are 290.707 eV [36], 301.8 eV [37], and 296.3 eV [38] for CH_4, CF_4, and CCl_4, respectively.

Our partial-wave expansion for the molecular orbitals and for the scattering wave functions included up to $l=15$ for CH_4 and up to $l=50$ for CF_4 and CCl_4. With this truncation, the error in the normalization of the methane molecular orbitals was less than 10^{-4}. For CF_4 the largest error was in the four F 1*s* orbitals (0.5%), while for CCl_4 the largest error was 13% for the Cl 1*s* orbitals. The error in the normalization of the C 1*s* orbitals, from which the photoelectron is removed, for all three molecules was less than 10^{-3}.

The differences between the results obtained with the dipole length and velocity forms were not significative for any of our calculations, indicating that our wave functions are well described. The results shown here were obtained using the mixed form. All cross sections shown below were converged with a maximum of seventh-order $[N/N]$ Padé approximants.

IV. RESULTS AND DISCUSSION

A. CH_4

The methane molecule presents a very smooth photoionization cross section, as shown in Fig. 1(a). The asymmetry parameter for this molecule is shown in Fig. 1(b). It is seen that the value of β approaches 2 for higher photon energies, which resembles the behavior of the β parameter expected for the ionization of an *s* orbital of an atom. This behavior is consistent with the fact that methane's electronic density is

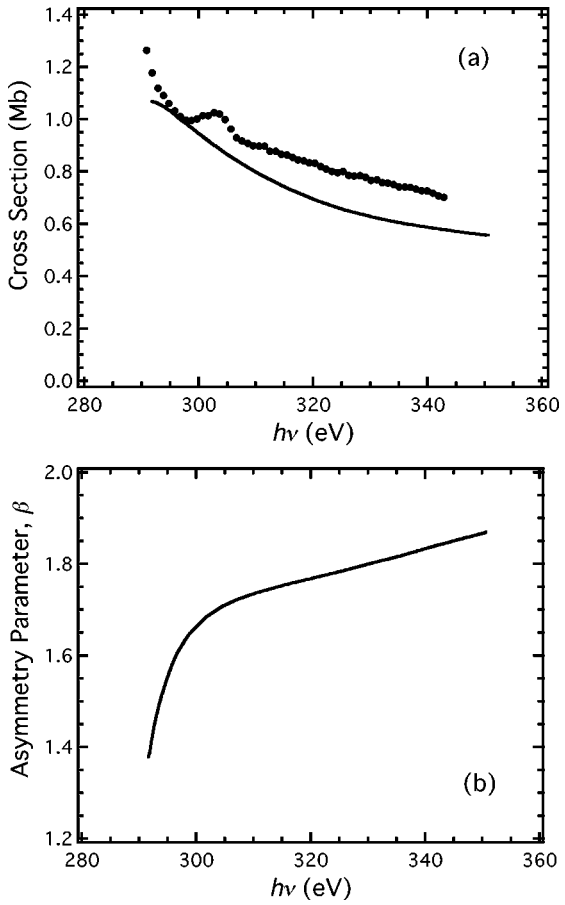

FIG. 1. (a) Cross sections for the C 1*s* photoionization of CH_4. Solid line, our results; circles, dipole absorption data of Hitchcock and co-workers [16,22]. (b) Computed asymmetry parameter for the C 1*s* photoionization of CH_4.

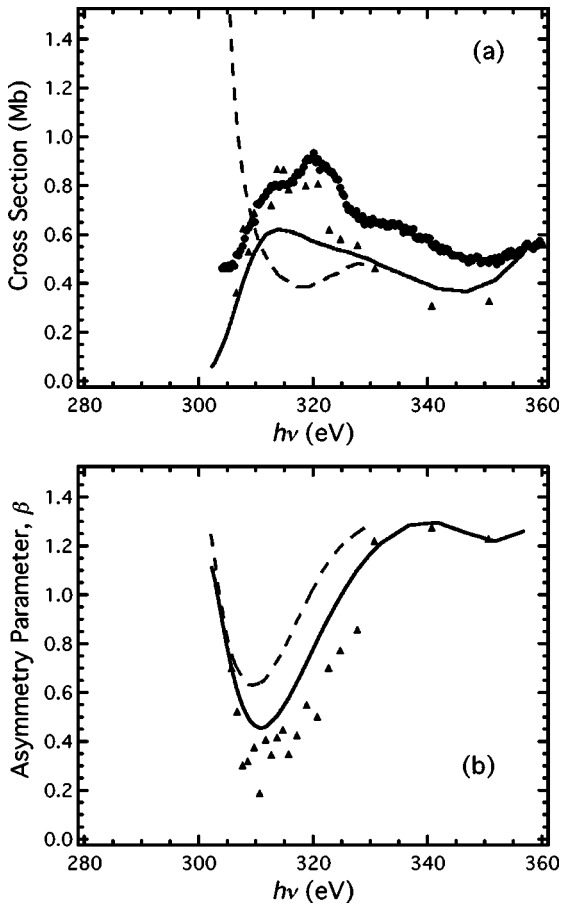

FIG. 2. (a) Cross sections for the C 1*s* photoionization of CF_4. Solid line, our results; dashed line, multiple-scattering model results [23]; circles, dipole absorption data of Hitchcock and co-workers [18,22]; triangles, experimental data of Truesdale *et al.* [24] normalized to the data of Hitchcock and co-workers [18,22] at 310.7 eV. (b) Asymmetry parameter for the C 1*s* photoionization of CF_4. The symbols and lines are the same as in (a).

almost spherically symmetric [39]. In Fig. 1(a), we have compared the computed photoionization cross section to the measured dipole absorption cross section [16,22]. The dipole absorption cross sections were obtained from small momentum transfer $(e,2e)$ cross sections that can yield the corresponding dipole photoabsorption cross section. With a suitable subtraction of the background absorption leading to states with lower ionization potentials an estimate of the total C 1*s* photoabsorption cross section can be obtained [22]. This total absorption cross section as shown in Fig. 1(a) is then an upper bound to the photoionization cross section. We note that there are no resonance features in the computed cross sections and thus the feature seen at about 302 eV in the experimental data is probably not due to a one-electron-scattering resonance, but is due to shake-up transitions as suggested by Wight and Brion [40].

B. CF_4

In Fig. 2(a) we show our calculated cross sections for the C 1*s* photoionization of CF_4 where we compare our results to the multiple-scattering model results of Stephens *et al.* [23] and to the experimental data of Truesdale *et al.* [24] (triangles) and of Hitchcock and co-workers [18,22] (circles). The relative cross sections of Truesdale *et al.* [24] were normalized to the electron-energy-loss results of Hitchcock and co-workers [18,22] at the photon energy of 310.7 eV. We see that our results are in good agreement with these two sets of experimental data, although the feature seen in the experiments near 320 eV is lacking in our calculations. This discrepancy is again probably due to the neglect of shake-up channels [41] in our calculation. The multiple-scattering model produces a curve with a very different behavior, especially near threshold, but for energies above 315 eV the results present about the same magnitude as ours.

From Fig. 2(a) it is seen that our cross sections for CF_4 reproduce the broad structure centered at about 315 eV, assigned by Truesdale *et al.* [24] as a shape resonance. In our full SVM calculation we can also compute the eigenphase sums for the scattering relative to the Coulomb scattering. The eigenphase sum in our calculation shows evidence of a very broad resonance with an energy $E_R = 308.3$ eV and a width of $\Gamma = 14.1$ eV when fit to a Breit-Wigner form [42]

$$\delta(E) = a + b(E_R - E) + c(E_R - E)^2 + \tan^{-1}\left[\frac{\Gamma}{2(E_R - E)}\right]. \tag{11}$$

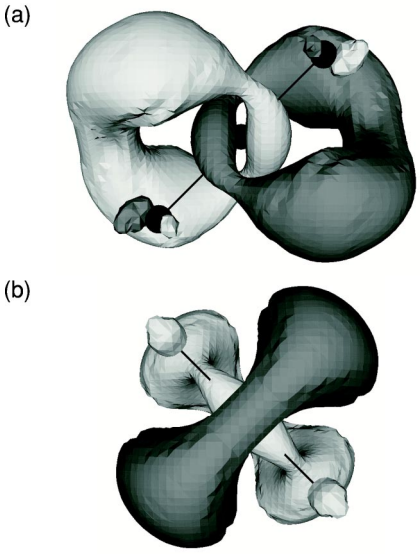

FIG. 3. Real part of the full resonant wave function for the resonance at 307.9 eV in the CF_4 cross sections from two different perspectives. Connected black spheres indicate the location of the nuclei; light and dark surfaces are constructed from the real part of the resonant wave function at constant positive and negative values of the wave function.

We have also examined this resonance with the ASME model and found a resonance with $E_R = 307.9$ eV and $\Gamma = 13.9$ eV. The three-dimensional picture of the wave function corresponding to this resonant state is shown in Fig. 3. The connected black spheres represent the atoms and the light and dark surfaces show parts of the wave function with opposite signs. We see that this state has significant amplitude between the F atoms on each side of the molecule. This resonant state appears to be a nonvalence state in agreement with the expectation discussed in the Introduction that all of the C $1s \rightarrow \sigma^*$(C-F) type states are located below the C $1s$ threshold [19,23].

Our results for the asymmetry parameter β for CF_4 are shown in Fig. 2(b), along with the multiple-scattering result of Stephens *et al.* [23] and the experimental results of Truesdale *et al.* [24]. Our curve presents a minimum at a photon energy of about 310 eV and is in very good agreement with experiment [24]. For energies above 335 eV the curve tends to a value of 1.3. The multiple-scattering results agree qualitatively well with the experiment and with our results.

C. CCl_4

The cross section curve for CCl_4 presents more defined resonance structures, as shown in Fig. 4(a). This molecule has an asymmetry parameter that does not seem to converge to any particular value [see Fig. 4(b)]. Comparing this result with our β parameters for the two other molecules, we see that heavier outer atoms produce more complex scattering dynamics.

We have also examined the resonances in CCl_4 using the

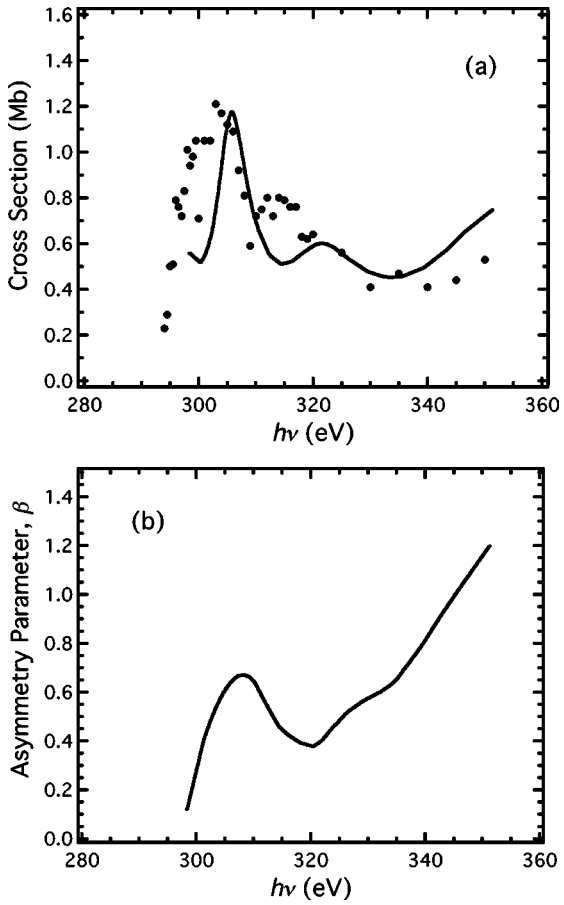

FIG. 4. (a) Cross sections for the C $1s$ photoionization of CCl_4. Solid line, our results; circles, dipole absorption data of Burton *et al.* [21] with background absorption removed to yield only the C $1s$ contribution. (b) Computed asymmetry parameter for the C $1s$ photoionization of CCl_4.

ASME model. We found three prominent resonances with $E_R = 304.3$ eV and $\Gamma = 3.5$ eV, $E_R = 313.0$ eV and $\Gamma = 8.3$ eV, and $E_R = 317.2$ eV and $\Gamma = 9.5$ eV. The lowest-energy resonance is responsible for the narrow resonance feature in the cross section seen in Fig. 4(a). The ASME results indicate that the two higher energies are overlapped and probably correspond to the feature seen at about 320 eV in Fig. 4(a).

In Figs. 5(a) and 5(b) we show a three-dimensional picture of the real part of the low-energy resonant wave function for CCl_4, from two different perspectives. Figure 5(b) indicates that this resonance has a significant contribution of d orbitals around the Cl atoms. In this picture two of the d orbitals are on Cl atoms above the plane containing the C atom (the upper right and lower left) while the other two d orbitals are on Cl atoms on a plane below the C atom. The dashed lines represent the approximate positions of the nodes of this wave function. Figure 6 presents only the $l = 5$ contribution of the resonant wave function. By comparing Figs. 5 and 6, one can see that the nodal surfaces asymptotically correspond to an $l = 5, m = 4$ real harmonic state where the z

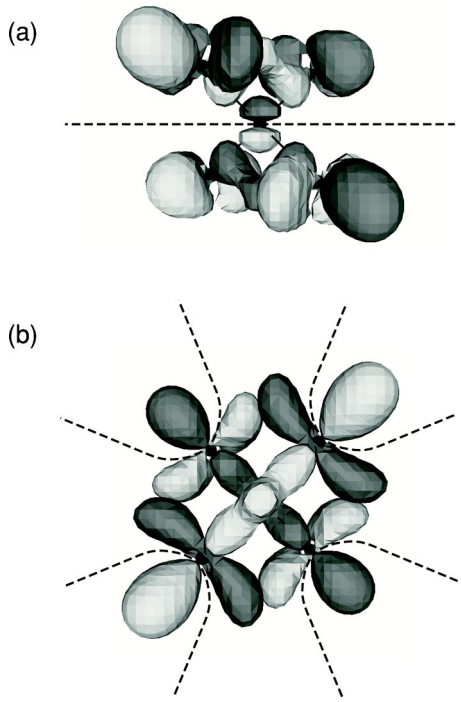

FIG. 5. Real part of the full resonant wave function for the resonance at 304.3 eV in the CCl_4 cross sections from two different perspectives. Connected black spheres indicate the location of the nuclei; light and dark surfaces are constructed from the real part of the resonant wave function at constant positive and negative values of the wave function; dashed lines indicate approximate positions of the nodes of this wave function. In the lower view, the nodal lines have a constant angular spacing of 45°.

axis is taken to be coming out of the plane in Figs. 5(b) and 6(b) and where the z axis is in the plane of Figs. 5(a) and 6(a) and is orthogonal to the nodal line. Comparing Figs. 5(b) and 6(b) we see that the upper-right and lower-left quadrants have the same phase in the two figures. The apparent difference in phase between the upper-left and lower-right quadrants of the figure comes from the fact that in the full wave function shown in Fig. 5 there are no lobes of the state in front of the plane containing the C atom, so that the lobes that are visible are those from behind the plane containing the C atom and thus have the same phase as the lobes in the upper-left and lower-right quadrants of the state shown in Fig. 6(b) that are behind the plane of the C atom. The relatively high-l characteristic of this state indicates that an angular-momentum barrier is responsible for the trapping of the state.

The other two resonances also have wave functions with strong d character. That there are three such resonances is consistent with the fact that from 20 d orbitals centered on the four Cl atoms one can construct three sets of t_2 orbitals. The identification of the continuum resonances in CCl_4 C 1s ionization with the d orbitals has been previously suggested by Zhang *et al.* [19]. Such d-orbital resonances have also been found previously in other systems containing second-row atoms [43].

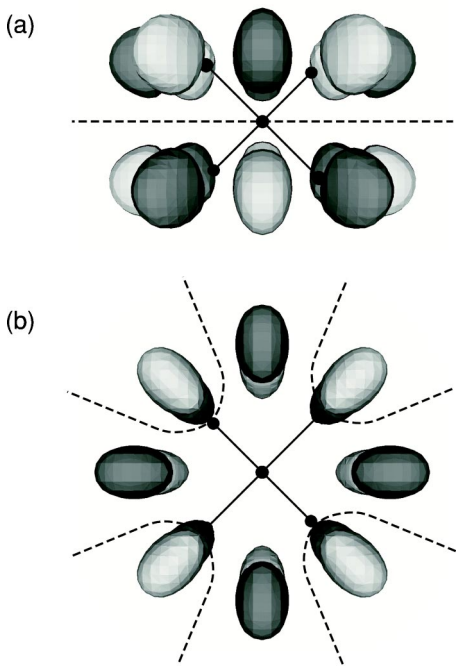

FIG. 6. Same as Fig. 5 but showing only the $l=5$ contribution.

V. CONCLUSIONS

We have studied the C 1s photoionization of CH_4, CF_4, and CCl_4 using the polyatomic Schwinger variational method with Padé corrections. Our computational model is a one-electron model so that we can only study the occurrence and nature of one-electron resonances, i.e., shape resonances. In CH_4 we find no such resonances leading to a structureless photoionization cross-section profile. The value of the photoelectron asymmetry parameter β is found to be very atomiclike at higher energies. In CF_4 and CCl_4 we do not expect to find any resonances that look like C $1s \rightarrow \sigma^*$(C-X) excitations since these states are known to occur below the C 1s ionization threshold. However, we do find shape resonances in the C 1s ionization of both CF_4 and CCl_4 which have significant effects on the cross sections in these systems. In CF_4 the resonant state is a very broad nonvalence state and in CCl_4 the resonant states all have d-like character in the region of the Cl atoms. In all the three systems considered there are features in the experimental cross sections which are not found in the one-electron calculations reported here. Thus these features are probably due to shake-up processes in these systems.

ACKNOWLEDGMENTS

The authors acknowledge the partial support from Brazilian agency Conselho Nacional de Desenvolvimento Científico e Tecnológico (CNPq). A.P.P.N. acknowledges the support from Fundação de Amparo à Pesquisa do Estado de São Paulo (FAPESP). R.R.L. would also like to acknowledge the support of the Robert A. Welch Foundation of Houston, Texas, under Grant No. A-1020, and the support of the Texas A&M University Supercomputing Facility.

[1] See, for example, L.G. Christophorou, J.K. Olthoff, and M.V.V.S. Rao, J. Phys. Chem. Ref. Data **25**, 1341 (1996); L.G. Christophorou and J.K. Olthoff, *ibid.* **28**, 967 (1999).
[2] P.J. Curry, S. Newell, and A.C. Smith, J. Phys. B **18**, 2303 (1985).
[3] K.Y. Kondrat'ev, Russ. Chem. Rev. **59**, 920 (1990).
[4] R.R. Lucchese and R.W. Zurales, Phys. Rev. A **44**, 291 (1991).
[5] J. Schirmer, M. Braunstein, and V. McKoy, Phys. Rev. A **44**, 5762 (1991).
[6] G. Bandarage and R.R. Lucchese, Phys. Rev. A **47**, 1989 (1993).
[7] M. Wells and R.R. Lucchese, J. Chem. Phys. **110**, 6365 (1999).
[8] P. Lin and R.R. Lucchese, J. Chem. Phys. **113**, 1843 (2000).
[9] R.E. Stratmann, G. Bandarage, and R.R. Lucchese, Phys. Rev. A **51**, 3756 (1995).
[10] L.E. Machado, L.M. Brescansin, M.A.P. Lima, M. Braunstein, and V. McKoy, J. Chem. Phys. **92**, 2362 (1990).
[11] L.E. Machado, M.-T. Lee, and L.M. Brescansin, J. Chem. Phys. **110**, 7228 (1999).
[12] L.M. Brescansin, M.A.P. Lima, L.E. Machado, M.-T. Lee, and V. McKoy, Braz. J. Phys. **27**, 468 (1997).
[13] A.P.P. Natalense and R.R. Lucchese, J. Chem. Phys. **111**, 5344 (1999); **112**, 501 (2000).
[14] F.A. Gianturco and R.R. Lucchese, Phys. Rev. A **64**, 32706 (2001).
[15] F.C. Brown, R.Z. Bachrach, and A. Bianconi, Chem. Phys. Lett. **54**, 425 (1978).
[16] A.P. Hitchcock and I. Ishii, J. Electron Spectrosc. Relat. Phenom. **42**, 11 (1987).
[17] K. Ueda, Y. Shimizu, H. Chiba, M. Okunishi, K. Ohmori, Y. Sato, E. Shigemasa, and N. Kosugi, J. Electron Spectrosc. Relat. Phenom. **79**, 441 (1996).
[18] I. Ishii, R. McLaren, A.P. Hitchcock, K.D. Jordan, Y. Choi, and M.B. Robin, Can. J. Chem. **66**, 2104 (1988).
[19] W. Zhang, T. Ibuki, and C.E. Brion, Chem. Phys. **160**, 435 (1992).
[20] S.-I. Itoh, S. Tanaka, and Y. Kayanuma, Phys. Rev. A **60**, 4488 (1999).
[21] G.R. Burton, W.F. Chan, G. Cooper, and C.E. Brion, Chem. Phys. **181**, 147 (1994).
[22] A.P. Hitchcock and D.C. Mancini, J. Electron Spectrosc. Relat. Phenom. **67**, 1 (1994).
[23] J.A. Stephens, D. Dill, and J.L. Dehmer, J. Chem. Phys. **84**, 3638 (1986).
[24] C.M. Truesdale, D.W. Lindle, P.H. Kobrin, U.E. Becker, H.G. Kerkhoff, P.A. Heimann, T.A. Ferrett, and D.A. Shirley, J. Chem. Phys. **80**, 2319 (1984).
[25] R.W. Zurales, E. Stratmann, S. Botting, and R.R. Lucchese, in *Photon and Electron Collisions with Atoms and Molecules*, edited by P.G. Burke and C.J. Joachain (Plenum, New York, 1997), p. 109.
[26] R.R. Lucchese and F.A. Gianturco, Int. Rev. Phys. Chem. **15**, 429 (1996).
[27] D. Loomba, S. Wallace, D. Dill, and J.L. Dehmer, J. Chem. Phys. **75**, 4546 (1981).
[28] R.R. Lucchese, K. Takatsuka, and V. McKoy, Phys. Rep. **131**, 147 (1986).
[29] F.A. Gianturco, R.R. Lucchese, and N. Sanna, J. Chem. Phys. **100**, 6464 (1994).
[30] S.L. Altmann, Proc. Cambridge Philos. Soc. **53**, 343 (1957).
[31] A.E. Hansen, Mol. Phys. **13**, 425 (1967).
[32] R.R. Lucchese, J. Chem. Phys. **92**, 4203 (1990).
[33] R.R. Lucchese, G. Raseev, and V. McKoy, Phys. Rev. A **25**, 2572 (1982).
[34] J. Schirmer, M. Braunstein, and V. McKoy, Phys. Rev. A **41**, 283 (1990).
[35] M.J. Frisch, G.W. Trucks, H.B. Schlegel, G.E. Scuseria, M.A. Robb, J.R. Cheeseman, V.G. Zakrzewski, J.A. Montgomery, Jr., R.E. Stratmann, J.C. Burant, S. Dapprich, J.M. Millam, A.D. Daniels, K.N. Kudin, M.C. Strain, O. Farkas, J. Tomasi, V. Barone, M. Cossi, R. Cammi, B. Mennucci, C. Pomelli, C. Adamo, S. Clifford, J. Ochterski, G.A. Petersson, P.Y. Ayala, Q. Cui, K. Morokuma, D.K. Malick, A.D. Rabuck, K. Raghavachari, J.B. Foresman, J. Cioslowski, J.V. Ortiz, A.G. Baboul, B.B. Stefanov, G. Liu, A. Liashenko, P. Piskorz, I. Komaromi, R. Gomperts, R.L. Martin, D.J. Fox, T. Keith, M.A. Al-Laham, C.Y. Peng, A. Nanayakkara, C. Gonzalez, M. Challacombe, P.M.W. Gill, B. Johnson, W. Chen, M.W. Wong, J.L. Andres, C. Gonzalez, M. Head-Gordon, E.S. Replogle, and J.A. Pople, computer code GAUSSION 98 (Revision A.7) (Gaussian, Pittsburgh, PA, 1998).
[36] L. Asplund, U. Gelius, S. Hedman, K. Helenelund, K. Siegbahn, and P.E.M. Siegbahn, J. Phys. B **18**, 1569 (1985).
[37] K. Siegbahn, C. Nordling, G. Johansson, J. Hedman, P.F. Hedén, K. Hamrin, U. Gelius, T. Bergmark, L.O. Werme, R. Manne, and Y. Baer, *ESCA Applied to Free Molecules* (North-Holland, Amsterdam, 1971), p. 89.
[38] T. Ohta and H. Kuroda, Bull. Chem. Soc. Jpn. **49**, 2939 (1976).
[39] M.T.do N. Varella, M.H.F. Bettega, and M.A.P. Lima, J. Phys. D **39**, 59 (1997).
[40] G.R. Wight and C.E. Brion, J. Electron Spectrosc. Relat. Phenom. **4**, 25 (1974).
[41] G.R. Wight and C.E. Brion, J. Electron Spectrosc. Relat. Phenom. **4**, 327 (1974).
[42] J.R. Taylor, *Scattering Theory* (Wiley, New York, 1972).
[43] R.E. Stratmann and R.R. Lucchese, J. Chem. Phys. **97**, 6384 (1992).
[44] D.R. Lide, *CRC Handbook of Chemistry and Physics*, 72th ed. (CRC, Boca Raton, 1992), pp. 9–17.
[45] L.E. Machado, M.-T. Lee, and L.M. Brescansin, Braz. J. Phys. **28**, 111 (1998).
[46] I. Iga, M.-T. Lee, M.G.P. Homem, L.E. Machado, and L.M. Brescansin, Phys. Rev. A **61**, 22 708 (2000).
[47] D.R. Lide, *CRC Handbook of Chemistry and Physics*, 80th ed. (CRC, Boca Raton, 2000), pp. 9–17.